Evaluation of Spin Lifetime in Strained UT2B Silicon-On-Insulator MOSFETs

Dmitri Osintsev, Viktor Sverdlov, and Siegfried Selberherr
Institute for Microelectronics, TU Wien, Gußhausstraße 27–29 / E360, A–1040 Wien, Austria
E-mail: {Osintsev|Sverdlov|Selberherr}@iue.tuwien.ac.at

***Abstract*—We investigate the surface roughness induced spin relaxation in scaled spin MOSFETs. We show that the regions in the momentum space, responsible for strong spin relaxation, can be efficiently removed by applying uniaxial strain. The spin lifetime in strained films can be improved by orders of magnitude, while the momentum relaxation time determining the electron mobility can only be increased by a factor of two.**

Keywords—surface-roughness relaxation; phonon relaxation; ultra-scaled SOI MOSFETs; shear strain

I. Introduction

Future microelectronic devices should exhibit a substantially reduced power consumption per operation. In addition, novel devices have to be smaller and faster. Spintronics considers novel devices which use the spin of electrons instead of the charge to perform an operation. A number of devices utilizing spin has already been proposed [1, 2]. Silicon is an ideal material for spintronic devices, because it is composed of nuclei with predominantly zero spin and is characterized by small spin-orbit coupling. Both factors favor to reduce spin relaxation. Understanding the details of the spin propagation in modern ultra-scaled silicon MOSFETs is urgently needed [3].

II. Model

A perturbative **k**·**p** approach [4–6] is suitable to describe the electron subband structure in the presence of strain and spin-orbit interaction in thin films. For the two [001] oriented valleys X_1 and $X_{2'}$ in a (001) silicon film the Hamiltonian is written in the vicinity of the X point along the k_z-axis in the Brillouin zone. The basis is conveniently chosen as [(X_1,↑), (X_1,↓), ($X_{2'}$, ↑), ($X_{2'}$,↓)], where ↑ and ↓ indicate the spin projection at the quantization z−axis. The effective **k**·**p** Hamiltonian reads as

$$H = \begin{bmatrix} H_1 & H_3 \\ H_3^\dagger & H_2 \end{bmatrix}, \tag{1}$$

where H_1, H_2, and H_3 are written as

$$H_1 = \left[\frac{\hbar^2 k_z^2}{2m_l} - \frac{\hbar^2 k_0 k_z}{m_l} + \frac{\hbar^2(k_x^2+k_y^2)}{2m_t} + U(z) \right] I, \tag{2}$$

$$H_2 = \left[\frac{\hbar^2 k_z^2}{2m_l} + \frac{\hbar^2 k_0 k_z}{m_l} + \frac{\hbar^2(k_x^2+k_y^2)}{2m_t} + U(z) \right] I, \tag{3}$$

$$H_3 = \begin{bmatrix} D\varepsilon_{xy} - \frac{\hbar^2 k_x k_y}{M} & (k_y - k_x i)\Delta_{SO} \\ (-k_y - k_x i)\Delta_{SO} & D\varepsilon_{xy} - \frac{\hbar^2 k_x k_y}{M} \end{bmatrix}. \tag{4}$$

Here I is the identity 2x2, m_t and m_l are the transversal and the longitudinal silicon effective masses, $k_0 = 0.15\times 2\pi/a$ is the position of the valley minimum relative to the X-point in unstrained silicon, ε_{xy} denotes the shear strain component, $M^{-1} \approx m_t^{-1} - m_0^{-1}$, Δ_{SO}=1.27meVnm [4], $U(z)$ is the confinement potential, and D = 14eV is the shear strain deformation potential.

We present an analytical approach to analyze surface roughness dominated spin relaxation in ultra-thin body and box (UT2B) SOI MOSFETs. By a unitary transformation the Hamiltonian (1) can be cast into a form in which spins with opposite orientations in different valleys are decoupled.

$$H = \begin{bmatrix} H_1 & H_3 \\ H_3 & H_2 \end{bmatrix} \tag{5}$$

H_1, H_2, and H_3 are written as

$$H_{1,2} = \left[\frac{\hbar^2 k_z^2}{2m_l} + \frac{\hbar^2(k_x^2+k_y^2)}{2m_t} + (-1)^j \delta + U(z) \right] I, \tag{6}$$

$$H_3 = \begin{bmatrix} \frac{\hbar^2 k_0 k_z}{m_l} & 0 \\ 0 & \frac{\hbar^2 k_0 k_z}{m_l} \end{bmatrix}, \tag{7}$$

with $\delta = \sqrt{\left(D\varepsilon_{xy} - \frac{\hbar^2 k_x k_y}{M}\right)^2 + \Delta_{SO}^2\left(k_x^2 + k_y^2\right)}$. Then the approach similar to that used for the two-band **k**·**p** Hamiltonian written in the vicinity of the X-point of the Brillouin zone for silicon films under uniaxial strain [6] is applicable to find the subband functions and subband energies.

The intrasubband and intersubband surface roughness scattering matrix elements are taken proportional to the square of the product of the subband function derivatives at the interface [7]. The relaxation time can be calculated by thermal averaging of the rate [3,4,7].

978-1-4673-5736-4/13/$31.00 ©2013 IEEE

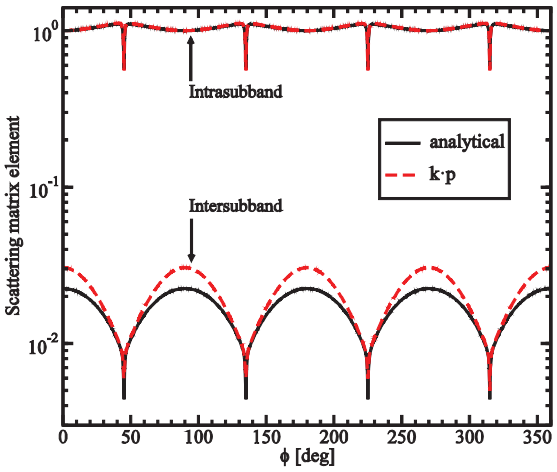

Fig. 1. Normalized intersubband and intrasubband scattering matrix elements as a function of the angle between an incident (k_x=0.25nm^{-1}, k_y=0.25nm^{-1}) and a reflected wave for $\varepsilon_{xy} = 0$.

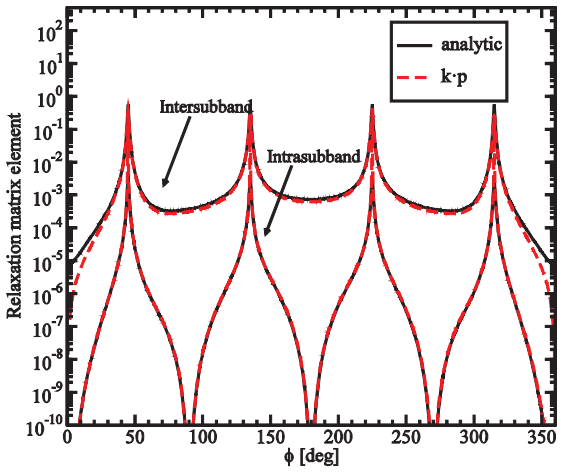

Fig. 2. Dependence of normalized spin relaxation matrix elements on the angle between an incident (k_x=0.25nm^{-1}, k_y=0.25nm^{-1}) and a reflected wave for $\varepsilon_{xy} = 0$.

$$\frac{1}{\tau} = \frac{\int \frac{1}{\tau(\mathbf{K_1})} f(\varepsilon)\left(1-f(\varepsilon)\right) d\mathbf{K_1}}{\int f(\varepsilon)\, d\mathbf{K_1}} \tag{8}$$

$$\int d\mathbf{K_1} = \int_0^{2\pi} \int_0^{\infty} \frac{|\mathbf{K_1}|}{\left|\frac{\partial \varepsilon(\mathbf{K_1})}{\partial \mathbf{K_1}}\right|} d\varphi\, d\varepsilon \tag{9}$$

The surface roughness induced momentum (spin) relaxation rate is calculated as

$$\frac{1}{\tau_{SR}(\mathbf{K_1})} = \frac{2(4)\pi}{\hbar} \sum_{i,j=1,2} \int_0^{2\pi} \pi \Delta^2 L^2 \frac{1}{\epsilon_{ij}^2(\mathbf{K_2}-\mathbf{K_1})} \cdot$$
$$\cdot \frac{\hbar^4}{4m_l^2} \left[\left(\frac{d\Psi_{i\mathbf{K_1}\sigma}}{dz} \right)^* \frac{d\Psi_{j\mathbf{K_2}\sigma(-\sigma)}}{dz} \right]_{z=\pm\frac{t}{2}}^2 \cdot$$
$$\cdot \exp\left(\frac{-(\mathbf{K_2}-\mathbf{K_1})^2 L^2}{4} \right) \frac{|\mathbf{K_2}|}{\left|\frac{\partial \varepsilon(\mathbf{K_2})}{\partial \mathbf{K_2}}\right|} \frac{1}{(2\pi)^2} d\varphi. \tag{10}$$

Here ε is the electron energy, $\mathbf{K_{1,2}}$ are the in-plane wave vectors before and after scattering, ϵ_{ij} is the dielectric permittivity, t is the film thickness, L is the autocorrelation length, Δ is the mean square value of the surface roughness fluctuations, $\Psi_{i\mathbf{K_1}}$ and $\Psi_{j\mathbf{K_2}}$ are the wave vectors, $f(\varepsilon)$ is the Fermi function, and σ is the spin projection to the [001] axis.

The electron-phonon scattering induced momentum relaxation rates are evaluated in a standard way [7]. The spin relaxation rate due to the transversal acoustic phonons is calculated as

$$\frac{1}{\tau_{TA}(\mathbf{K_1})} = \frac{2\pi k_B T}{\hbar \rho v_{TA}^2} \sum \int_0^{2\pi} \frac{|\mathbf{K_2}|}{\left|\frac{\partial \varepsilon(\mathbf{K_2})}{\partial \mathbf{K_2}}\right|} \cdot$$
$$\cdot \left[1 - \frac{\frac{\partial \varepsilon(\mathbf{K_2})}{\partial \mathbf{K_2}} f(\varepsilon(\mathbf{K_2}))}{\frac{\partial \varepsilon(\mathbf{K_1})}{\partial \mathbf{K_1}} f(\varepsilon(\mathbf{K_1}))} \right] \cdot$$
$$\cdot \frac{1}{2} \int_0^t \int_0^t \exp\left(-\sqrt{q_x^2+q_y^2}|z-z'|\right) \cdot$$
$$\cdot \left[\Psi^\dagger_{\mathbf{K_2}-\sigma}(z) M_{TA} \Psi_{\mathbf{K_1}\sigma}(z) \right] \left[\Psi^\dagger_{\mathbf{K_2}-\sigma}(z') M_{TA} \Psi_{\mathbf{K_1}\sigma}(z') \right] \cdot$$
$$\cdot \left[\sqrt{q_x^2+q_y^2} - \frac{8q_x^2 q_y^2 - (q_x^2+q_y^2)^2}{q_x^2+q_y^2} |z-z'| \right] dz dz', \tag{11}$$

k_B is the Boltzmann constant, T is the temperature, ρ =2329$\frac{\mathrm{kg}}{\mathrm{m}^3}$ is the silicon density, v_{TA}=5300$\frac{\mathrm{m}}{\mathrm{s}}$ is the transversal phonons velocity, $(q_x, q_y) = \mathbf{K_1} - \mathbf{K_2}$, the matrix M_{TA} is

$$M_{TA} = \begin{bmatrix} 0 & 0 & \frac{D_{xy}}{2} & 0 \\ 0 & 0 & 0 & \frac{D_{xy}}{2} \\ \frac{D_{xy}}{2} & 0 & 0 & 0 \\ 0 & \frac{D_{xy}}{2} & 0 & 0 \end{bmatrix}. \tag{12}$$

Here D_{xy}=14eV is the shear deformation potential.

The intravalley spin relaxation rate due to the longitudinal acoustic phonons is calculated as

$$\frac{1}{\tau_{LA}(\mathbf{K_1})} = \frac{2\pi k_B T}{\hbar \rho v_{LA}^2} \sum \int_0^{2\pi} \frac{|\mathbf{K_2}|}{\left|\frac{\partial \varepsilon(\mathbf{K_2})}{\partial \mathbf{K_2}}\right|} \cdot$$
$$\cdot \left[1 - \frac{\frac{\partial \varepsilon(\mathbf{K_2})}{\partial \mathbf{K_2}} f(\varepsilon(\mathbf{K_2}))}{\frac{\partial \varepsilon(\mathbf{K_1})}{\partial \mathbf{K_1}} f(\varepsilon(\mathbf{K_1}))} \right] \cdot$$
$$\cdot \frac{1}{2} \int_0^t \int_0^t \exp\left(-\sqrt{q_x^2+q_y^2}|z-z'|\right) \cdot$$
$$\cdot \left[\Psi^\dagger_{\mathbf{K_2}-\sigma}(z) M_{TA} \Psi_{\mathbf{K_1}\sigma}(z) \right] \left[\Psi^\dagger_{\mathbf{K_2}-\sigma}(z') M_{TA} \Psi_{\mathbf{K_1}\sigma}(z') \right] \cdot$$
$$\cdot \frac{4q_x^2 q_y^2}{\left(\sqrt{q_x^2+q_y^2}\right)^3} \left[\sqrt{q_x^2+q_y^2}|z-z'| + 1 \right] dz dz'. \tag{13}$$

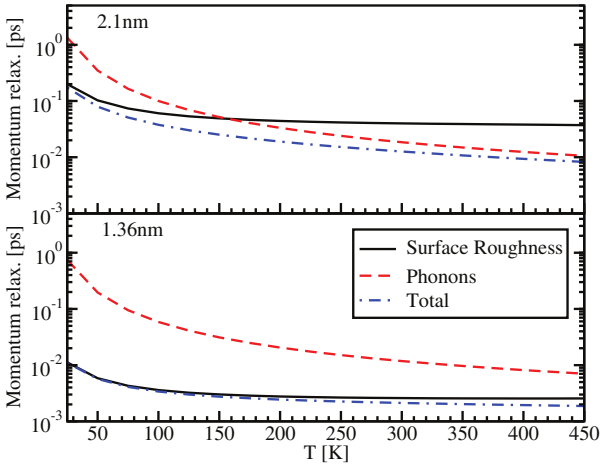

Fig. 3. Dependence of the momentum relaxation time induced by surface roughness (SR), phonons, and total momentum relaxation time on temperature for two different thicknesses, ε_{xy}=0, and electron concentration $1.29\cdot10^{12}$cm^{-2}.

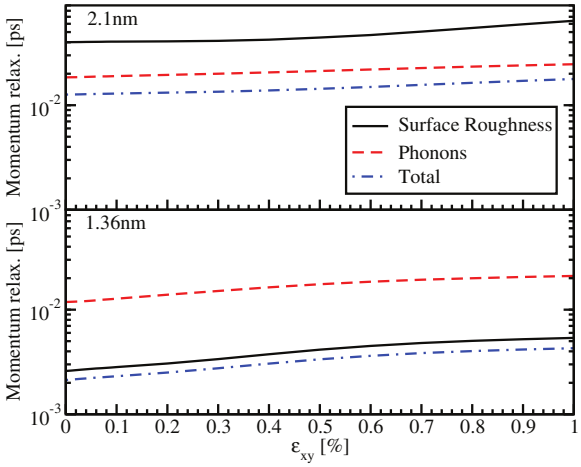

Fig. 4. Dependence of the momentum relaxation time induced by surface roughness, phonons, and total momentum relaxation time on shear strain for 1.36nm and 2.1nm film thicknesses, for T=300K, and electron concentration $1.29\cdot10^{12}$cm^{-2}.

Here v_{LA}=8700$\frac{\text{m}}{\text{s}}$ is the speed of the longitudinal phonons.

The intervalley spin relaxation rate contains the Elliot and Yafet contributions [3], which are calculated in the following way

$$\frac{1}{\tau_{LA}(\mathbf{K_1})} = \frac{2\pi k_B T}{\hbar\rho v_{LA}^2}\sum\int_0^{2\pi}\frac{|\mathbf{K_2}|}{\left|\frac{\partial\varepsilon(\mathbf{K_2})}{\partial\mathbf{K_2}}\right|}\cdot$$
$$\cdot\left[1-\frac{\frac{\partial\varepsilon(\mathbf{K_2})}{\partial\mathbf{K_2}}f(\varepsilon(\mathbf{K_2}))}{\frac{\partial\varepsilon(\mathbf{K_1})}{\partial\mathbf{K_1}}f(\varepsilon(\mathbf{K_1}))}\right]\cdot$$
$$\cdot\frac{1}{2}\int_0^t\left[\Psi^{\dagger}_{\mathbf{K_2}-\sigma}(z)M_{LA}\Psi_{\mathbf{K_1}\sigma}(z)\right]^*\cdot$$
$$\cdot\left[\Psi^{\dagger}_{\mathbf{K_2}-\sigma}(z)M_{LA}\Psi_{\mathbf{K_1}\sigma}(z)\right]dz. \quad (14)$$

The matrix M_{LA} is written as

$$M_{LA} = \begin{bmatrix} M_{ZZ} & M_{SO} \\ M_{SO}^{\dagger} & M_{ZZ} \end{bmatrix}, \quad (15)$$

$$M_{ZZ} = \begin{bmatrix} D_{ZZ} & 0 \\ 0 & D_{ZZ} \end{bmatrix}, \quad (16)$$

$$M_{SO} = \begin{bmatrix} 0 & D_{SO}\left(K_{SO_y} - iK_{SO_x}\right) \\ D_{SO}\left(-K_{SO_y} - iK_{SO_x}\right) & 0 \end{bmatrix}. \quad (17)$$

Here $\left(K_{SO_x}, K_{SO_y}\right) = \mathbf{K_1} + \mathbf{K_2}$, D_{ZZ}=12eV, D_{SO}=15meV/k$_0$ with $k_0 = 0.15\times2\pi/a$ defined as the position of the valley minimum relative to the X-point in unstrained silicon [3].

III. Results and Discussion

Figure 1 shows intersubband and intrasubband scattering matrix elements normalized to the intrasubband scattering matrix elements at zero strain as a function of the angle between the wave vectors $\mathbf{K_1}$ and $\mathbf{K_2}$. Results obtained by solving numerically the $\mathbf{k}\cdot\mathbf{p}$ Hamiltonian (1) with a square well potential and by analytical treatment (5) are in good agreement. Figure 2 shows the spin relaxation matrix elements due to surface roughness scattering. Intersubband spin relaxation is expected to be stronger than the intrasubband one. A strong dependence of the intersubband and the intrasubband relaxation matrix elements on both $\mathbf{K_1}$ and $\mathbf{K_2}$ demands a large amount of computational resources in order to compute the relaxation times (10, 11, 13, 14). Because of the sharp picks shown in Figure 2 a multi-dimensional integral over the energy and different directions of the wave vectors enforces to evaluate the wave functions and their derivatives at around a billion points in momentum space. To handle this complexity a highly parallelized approach has been developed.

Figure 3 shows the dependence of the momentum relaxation time on temperature. The contributions from the surface roughness and phonons to the total momentum relaxation time are shown. The phonon contribution to the total relaxation time depends strongly on temperature. Thus, for the film thicknesses 2.1nm and 1.36nm, the surface roughness is the dominant mechanism of the momentum relaxation at low temperatures. For a temperature around 150K for the film of 2.1nm thickness the surface roughness and phonon induced momentum relaxation mechanisms yield similar contributions to the total momentum relaxation time. At room temperature the total momentum relaxation time is mainly determined by phonon scattering. However, Figure 3 shows that for the thinner film the dominant relaxation mechanism is the surface roughness in the whole range of investigated temperatures. Thus, the dominant relaxation mechanism strongly depends on the film thickness. Indeed, the surface roughness limited momentum relaxation increases by more than an order of magnitude because of the expected t^{-6} dependence [7, 8], while the phonon limited momentum relaxation is

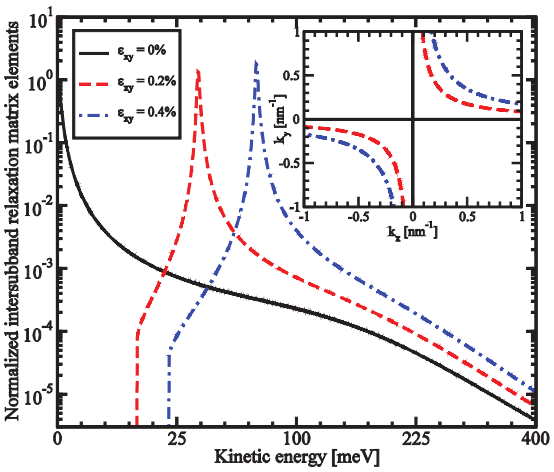

Fig. 5. Normalized intersubband relaxation matrix elements as a function of the conduction electrons kinetic energy in [110] direction. The inset shows the positions of the hot spots for different values of shear strain.

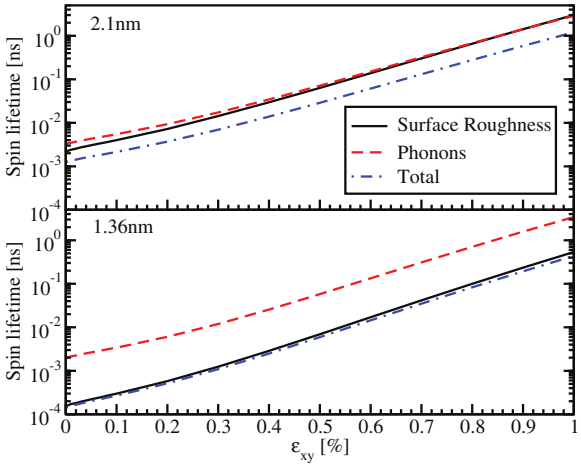

Fig. 6. Dependence of the spin lifetime induced by surface roughness, phonons, and total momentum relaxation time on shear strain for two different film thicknesses, for T=300K, and electron concentration $1.29 \cdot 10^{12} cm^{-2}$.

characterized by a weaker thickness dependence and does not increase as significantly as the surface roughness induced relaxation, when the thickness is decreased from 2.1nm to 1.36nm. Therefore, for the thickness 1.36nm the surface roughness induced momentum relaxation is the dominant mechanism for the whole range of considered temperatures, in agreement with Figure 3.

Figure 4 shows the dependence of the different mechanisms of the momentum relaxation together with the total momentum relaxation time on shear strain. The improvement of the momentum relaxation time due to shear strain is around 60% for the film thickness of 2.1nm and around 110% for the film thickness 1.36nm. The phonons limited momentum relaxation time improves by around 45% for 2.1nm and 90% for 1.36nm. The surface roughness limited momentum relaxation time increases by 120% for 2.1nm and for 1.36nm. Since the surface roughness mechanism is dominant for the film thickness 1.36nm, the increase of the total momentum relaxation time is higher for 1.36nm than for 2.1nm film thickness. Combined with the strain induced transport effective mass decrease it results in an even better mobility improvement supporting the use of uniaxial tensile strain as the mobility booster in fully depleted ultra-thin SOI MOSFETs.

Figure 5 displays the surface roughness spin relaxation matrix elements normalized to the scattering matrix elements at zero strain. To evaluate the electron spin relaxation we take the matrix elements on the wave functions with the opposite spin projections $\sigma' = -\sigma$ corresponding to the spin flip events. For an unstrained film points characterized by a large mixing between the spin-up and spin-down states from the opposite valleys ("hot spots") are along the [100] and [010] directions (inset in Figure 5). Shear strain pushes the "hot spots" to higher energies away from the subband minima. This leads to a strong increase of the spin lifetime shown in Figure 6. Therefore shear strain routinely used to boost mobility can significantly reduce spin relaxation in UT2B SOI MOSFETs.

IV. Conclusion

By utilizing a **k·p** approach which includes the spin-orbit interaction effects we found the subband wave functions and subband energies in (001) thin silicon films. We have shown that the momentum relaxation time can be improved by almost a factor of two for ultra-thin films. We have demonstrated a strong, several orders of magnitude, increase of spin lifetime in strained silicon films. Thus shear strain used to boost mobility can also be used to increase spin lifetime.

Acknowledgment

This work is supported by the European Research Council through the grant #247056 MOSILSPIN. The computational results have been achieved in part using the Vienna Scientific Cluster (VSC).

References

[1] S. Sugahara and J. Nitta, Spin transistor electronics: An overview and outlook, Proceedings of the IEEE, 98(12),

[2] S. Datta and B. Das, Electronic analog of the electro-optic modulator, Applied Physics Letters, 56, 665 (1990).

[3] Y. Song, H. Dery, Analysis of phonon-induced spin relaxation processes in silicon, Physical Review B, 86, 085201 (2012).

[4] P. Li, H. Dery, Spin-orbit symmetries of conduction electrons in silicon, Physical Review Letters, 107, 107203 (2011).

[5] G.L. Bir, G.E. Pikus, Symmetry and strain-induced effects in semiconductors. New York/Toronto: J. Wiley & Sons 1974.

[6] V. Sverdlov, Strain-induced effects in advanced MOSFETs. Wien - New York. Springer 2011.

[7] M. V. Fischetti et al., Six-band k·p calculation of hole mobility in silicon inversion layers: Dependence on surface orientation, strain, and silicon thickness, Journal of Applied Physics, 94, 1079 (2003).

[8] S. Jin, M.V. Fischetti, T.-W. Tang, *Modeling of surface roughness scattering in ultrathin-body SOI MOSFETs*, IEEE Transaction Electron Devices, 54(9), 2191–2202 (2007).